



SAKARYA ÜNİVERSİTESİ

# FEN BİLİMLERİ ENSTİTÜSÜ DERGİSİ

Sakarya University Journal of Science  
SAUJS

e-ISSN 2147-835X | Period Bimonthly | Founded: 1997 | Publisher Sakarya University |  
<http://www.saujs.sakarya.edu.tr/en/>

Title: Comparison of Polyol and Hydrothermal Methods for Synthesis of Zinc Oxide Nanoparticles

Authors: Elif ERÇARIKCI, Murat ALANYALIOĞLU

Received: 2020-12-07 14:00:25

Accepted: 2020-12-10 16:49:57

Article Type: Research Article

Volume: 25

Issue: 1

Month: February

Year: 2021

Pages: 175-181

How to cite

Elif ERÇARIKCI, Murat ALANYALIOĞLU; (2021), Comparison of Polyol and Hydrothermal Methods for Synthesis of Zinc Oxide Nanoparticles. Sakarya University Journal of Science, 25(1), 175-181, DOI:

<https://doi.org/10.16984/saufenbilder.836613>

Access link

<http://www.saujs.sakarya.edu.tr/en/pub/issue/58068/836613>

New submission to SAUJS

<https://dergipark.org.tr/en/journal/1115/submission/step/manuscript/new>

## Comparison of Polyol and Hydrothermal Methods for Synthesis of Zinc Oxide Nanoparticles

Elif ERÇARIKCI<sup>1</sup>, Murat ALANYALIOĞLU\*<sup>2</sup>

### Abstract

Zinc oxide (ZnO) is an inorganic semiconductor compound with a direct band gap of 3.3 eV and is mainly used as additive in many technological applications such as cosmetic, food, and cement. The functionality of ZnO strongly depends on the particle size, crystallinity, and shape. In this work, ZnO nanoparticles (ZnONPs) were prepared using two different routes: polyol and hydrothermal processes. The products were compared using scanning electron microscopy, transmission electron microscopy, X-Ray diffraction, Fourier transform infrared spectroscopy, and UV-Vis. absorption spectroscopy techniques. Additionally, hydrothermal method was performed at three temperature values of 100, 120, and 150 °C and the effect of temperature on the hydrothermal synthesis of ZnONPs was also discussed in this study.

**Keywords:** ZnO, polyol method, hydrothermal method.

### 1. INTRODUCTION

Metal oxide nanoparticles are important materials for many technological applications like cement, cosmetic, food, and dyeing. Because the most of metal oxides demonstrate a semiconductor property, they are preferred as dopant to produce batteries [1-3], supercapacitors [4,5], sensors [6,7], solar cells [8,9], membranes [7,10] and so on.

Zinc oxide (ZnO) absorbs sunlight efficiently and it is especially preferred for solar cell applications [8,9] as well as TiO<sub>2</sub>. The quality parameters such as crystallinity, particle size, and shape of ZnO are required to be controlled for such applications. There are various techniques to synthesize zinc oxide nanoparticles (ZnONPs) in the literature

e.g. atomic layer deposition [3,11], electrodeposition [12], thermal evaporation [13], sol-gel [14], and precipitation [15] methods.

Complicated devices and specialty are not essential for precipitation method. Hence, this method is in prevalent use. To adjust the physical, optical, and electrical properties of ZnONPs, precipitation can be applied using various approaches such as polyol [16] and hydrothermal [17] procedures, in which high temperature is applied using reducing agents and stabilizers.

In this study, ZnONPs were synthesized using both polyol and hydrothermal procedures and their morphological, crystallographic, chemical, and optical properties were compared as well as

<sup>1</sup> Ataturk University, Faculty of Science, Erzurum, Turkey.

ORCID: <https://orcid.org/0000-0002-8490-1644> E-Mail: [elif.ercarikci@atauni.edu.tr](mailto:elif.ercarikci@atauni.edu.tr)

\*Corresponding Author: [malanya@atauni.edu.tr](mailto:malanya@atauni.edu.tr)

<sup>2</sup> Ataturk University, Faculty of Science, Erzurum, Turkey. ORCID: <https://orcid.org/0000-0002-2223-7303>

the influence of temperature on the hydrothermal process.

## 2. EXPERIMENTAL SECTION

All reagents were of analytical grade and all synthetic procedures were applied in aqueous solutions using ultrapure water. For the synthesis of ZnONPs by polyol method, 30 mL of diethylene glycol (DEG) solution including 4.0 mM poly(vinyl)pyrrolidone (PVP) was prepared at room temperature.  $\text{Zn}(\text{CH}_3\text{COO})_2 \cdot 6\text{H}_2\text{O}$  was added into this solution to a final concentration of 0.1 M and heated to 180 °C. Distilled water was injected into the solution at a constant rate of 1 ml/s. The mixture has started to become milky due to precipitation of ZnONPs. The precipitation was supplied for 30 min while temperature was kept constant at 180 °C. Thus, the suspension was allowed to reach room temperature, ZnONPs were filtrated, cleaned with ethanol and distilled water, respectively, and then dried overnight at room temperature [16]. This product was quoted as ZnONPs-po

Hydrothermal synthesis of ZnONPs was accomplished by the following procedure [17]. 5 mL of 1.0 M KOH solution was added to 25 mL of DEG under magnetic stirring. 10 mL of 0.4 M  $\text{Zn}(\text{NO}_3)_2 \cdot 6\text{H}_2\text{O}$  and 0.59 g of hexadecyl trimethylammonium bromide (CTAB) was also inserted into this solution and then stirred for 10 min. This dispersion was placed into autoclave and heated at different constant temperature values of 100, 120 and 150 °C for 3 h to investigate the effect of temperature on the formation of ZnONPs. When the precipitation reactions were finished, the suspensions were cooled at room temperature. The white ZnONPs powders were separated by filtration, cleaned with ethanol and distilled water, respectively, and dried overnight at room temperature. These precipitates were named as ZnONPs-ht

In these synthesis procedures, DEG was used as reducing agent, while PVP and CTAB were serving as stabilizer role to confine the particle size of ZnO. For the characterization of produced ZnONPs, morphological, optical, chemical, and crystallographic analyses were performed.

Morphological information was collected using Zeiss scanning electron microscopy (SEM) and Hitachi transmission electron microscopy (TEM). Optical and chemical analysis of the ZnONPs were provided by Shimadzu UV-Vis. spectrophotometer and Perkin-Elmer Fourier transform infrared (FTIR) system. The samples were prepared as KBr pellets for FTIR analysis. Crystallographic information of the samples were collected using Rigaku brand X-ray diffraction instrument.

## 3. RESULTS AND DISCUSSION

Morphological characterization of the synthesized ZnONPs was performed using SEM and TEM techniques. Fig. 1.a shows SEM image of ZnONPs-po with a very large ball-shaped view. The particle size of ZnONPs-po ranges between 400 nm and 2 μm.

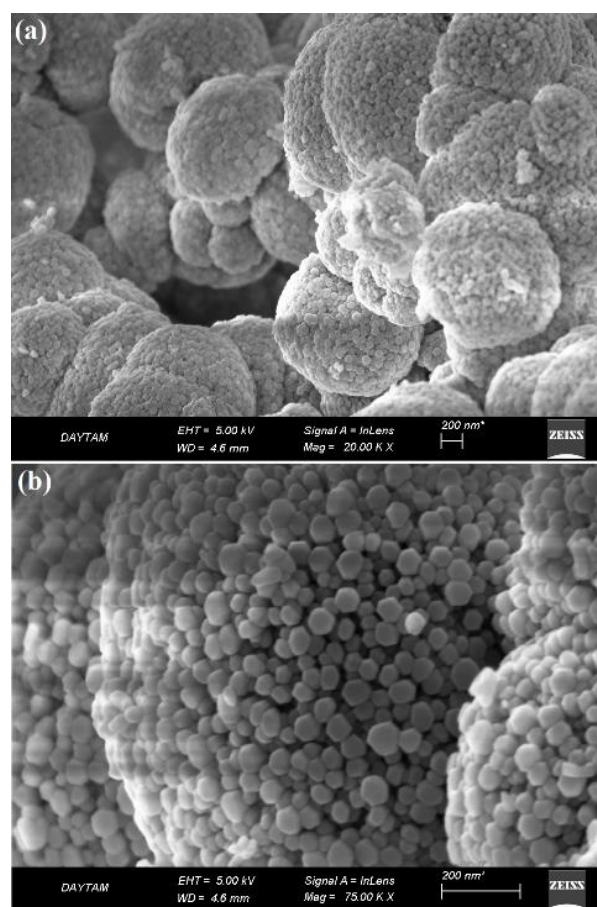


Figure 1 Low (a) and high (b) magnification SEM images of ZnONPs-po

When we focus on these large particles, it is obvious that there are many highly ordered sub-crystals as illustrated in Fig. 1.b. These hexagonal shaped sub-units are distributed so homogeneously and mean particle size is around 70 nm.

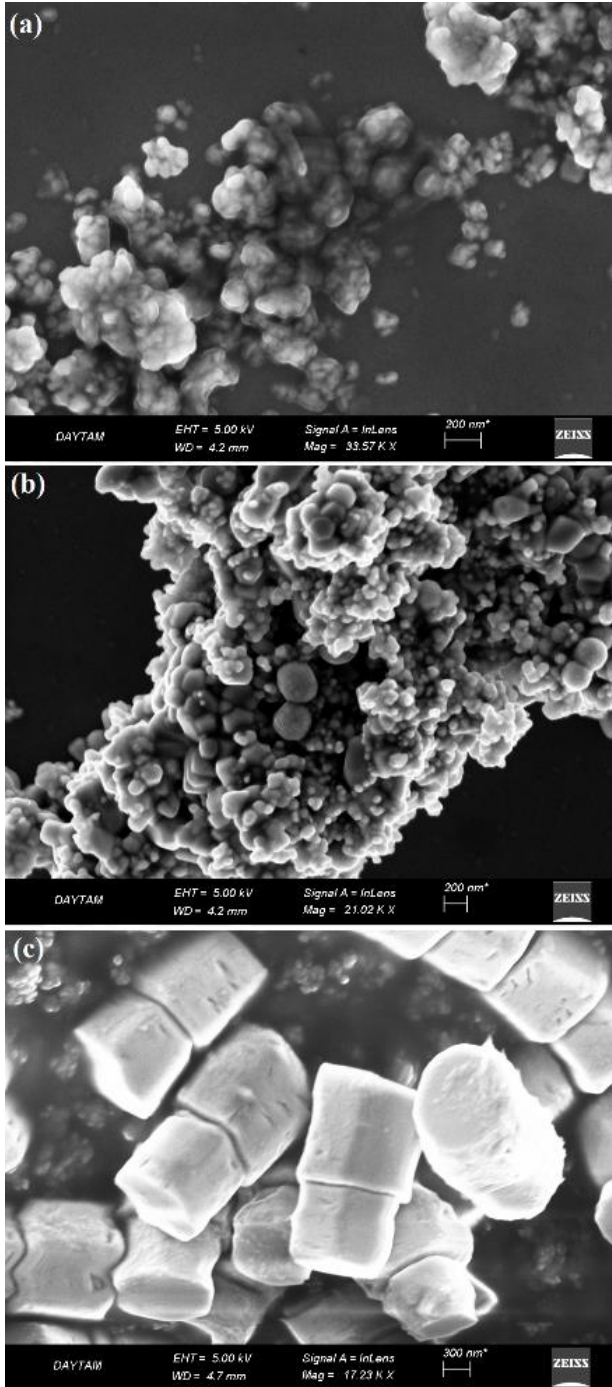


Figure 2 SEM images of ZnONPs-ht prepared at 100 °C (a), 120 °C (b), and 150 °C (c).

Fig. 2 demonstrates SEM images of ZnONPs-ht structures synthesized at 100, 120, and 150 °C. This figure indicates that ZnONPs-ht reveal a totally distinct surface structure at all of the studied temperature values. It should also be noted from Fig. 2 that surface appearance of ZnONPs-ht changes depending on the applied temperature. At 100 and 120 °C, SEM images of ZnONPs-ht reflect aggregated particles with lower crystalline view when compared to ZnONPs-po. Particle size of ZnONPs-ht was calculated as 50 nm for 100 °C (Fig. 2.a). It is observed in Fig. 2.b that more aggregated particles are seen for 120 °C and some larger particles arise on the surface. Hydrothermal synthesis at 150 °C results in a totally divergent formation. Interestingly, very large screw-like crystals with a few  $\mu\text{m}$  particle size constitute on the aggregated small particles.

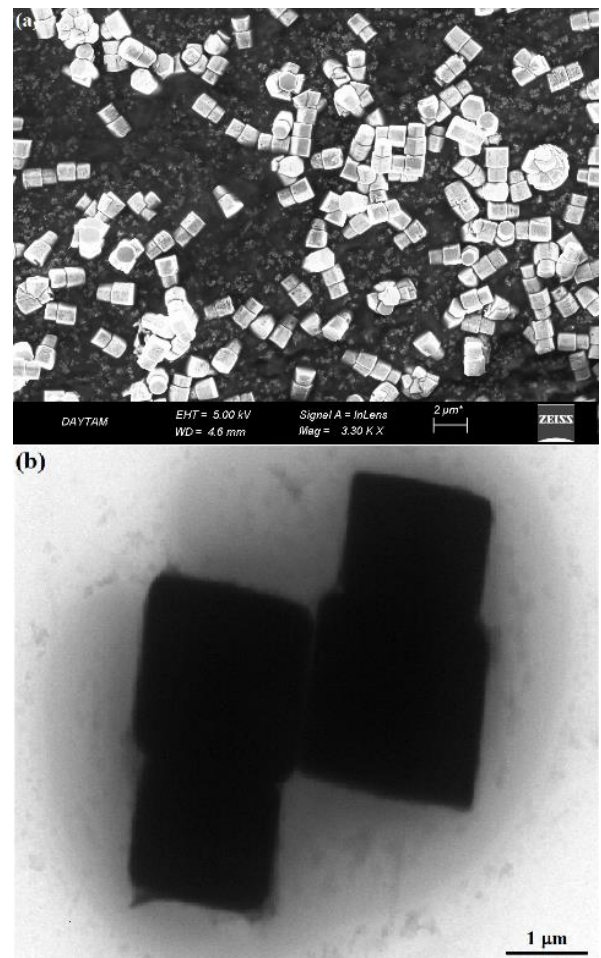


Figure 3 SEM (a) and TEM (b) images of ZnONPs-ht prepared at 150 °C.

Fig. 3.a represents a low magnification SEM image of these ZnONPs-ht crystals, in which screw-like crystals are homogeneously distributed on the surface. Fig. 3.b also shows a TEM image of ZnONPs-ht synthesized at 150 °C. This figure implies that large crystals reveal a very low transparency and the dimensions of these shapes are approximately  $2.5 \mu\text{m} \times 4.0 \mu\text{m}$ .

To investigate crystallographic properties of the prepared ZnONPs, powder XRD analysis was carried out as represented in Fig. 4. XRD spectrum of ZnONPs-po contains different peaks at  $2\theta$  values of  $31.8^\circ$ ,  $34.5^\circ$ ,  $36.3^\circ$ ,  $47.6^\circ$ ,  $56.5^\circ$ ,  $62.7^\circ$ , and  $67.8^\circ$  for the diffractions of 100, 002, 101, 102, 110, 103, and 200 depending on the joint committee on powder diffraction standards (JCPDS) card number of 36-1451 [18]. In Fig. 4, same peaks are observed for ZnONPs-ht samples prepared at different temperatures.

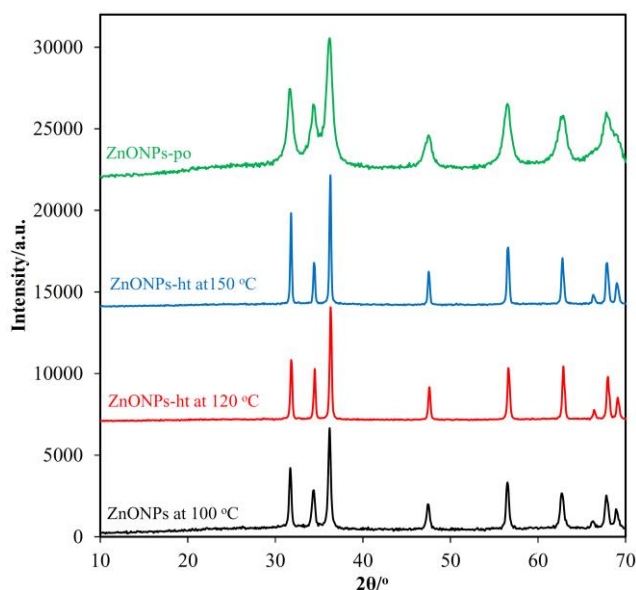


Figure 4 XRD data of ZnONPs prepared by polyol and hydrothermal methods

SEM analysis supplied visible particle size of the samples but it is clear that particle sizes for all samples are not uniform. XRD data provides mean particle size information depending on the Scherrer equation [19]. Using the most intensive peak, we have calculated particle size of ZnONPs-

po as 120 nm, while particles sizes of ZnONPs-ht samples are 345, 415, and 520 nm for 100, 120, and 150 °C, respectively. It can be concluded from both SEM and XRD results that polyol process provides lower particle size and particle size increases by rising the applied temperature for hydrothermal process.

Fig. 5 displays FTIR spectra of ZnONPs-po and ZnO-NPs-ht. ZnONPs-po spectrum is very close to that of previous publications [20-22] and includes individual peaks at  $507$ ,  $1049$ ,  $1388$ ,  $1607$ ,  $2978$ , and  $3398 \text{ cm}^{-1}$ , corresponding to vibration of Zn-O, C-N, C-H, C=O, C-H, and –OH groups, respectively. It is obvious that ZnONPs-po are covered with PVP molecules, those are immobilized to ZnONPs-po during the synthesis step. The FTIR spectrum of ZnONPs-ht exhibits almost similar peaks of spectrum of ZnONPs-po but two differences should be remarked. First difference is the arising of an intensive peak at  $550 \text{ cm}^{-1}$ , which is assigned to vibration of C-Br of CTAB [23], which is used as stabilizer. Second discrepancy is the diminishing the intensity of C=O bond, which is due to the absence of carbonyl group in the CTAB structure. The FTIR results ratify the successful synthesis of both ZnONPs structures by applied synthetic procedures.

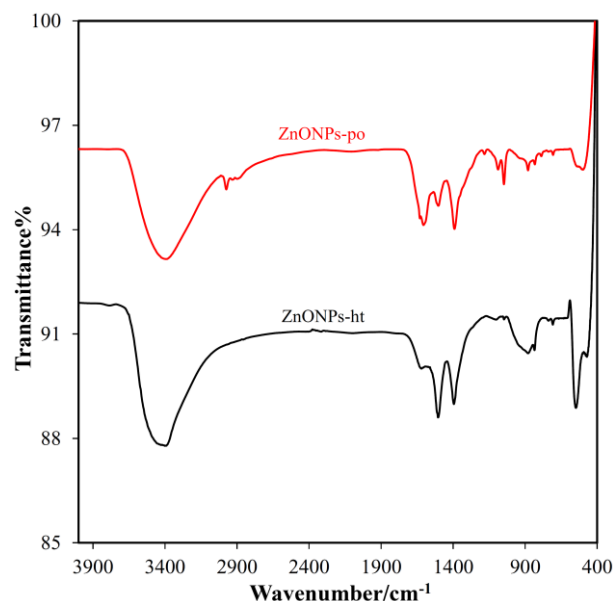


Figure 5 FTIR spectra of ZnONPs prepared by polyol and hydrothermal (150 °C) methods

Optical properties of ZnONPs were analyzed using UV-Vis. absorption spectroscopy (Fig. 6). For ZnONPs-po and ZnONPs-ht dispersions, absorption maxima were observed at 376 and 371 nm corresponding to band gap values of 3.30 and 3.34 eV, respectively based on the following equation.

$$E = \frac{h c}{\lambda_{abs}}$$

where  $h$  is Planck constant ( $6.62 \times 10^{-34}$  J.s),  $c$  is the velocity of light ( $3 \times 10^8$  m.s $^{-1}$ ) and  $\lambda_{abs}$  is the absorption wavelength [22,24]. Calculated band gap values of both samples show that applied synthesis procedures yielded the bulk structure of ZnONPs.

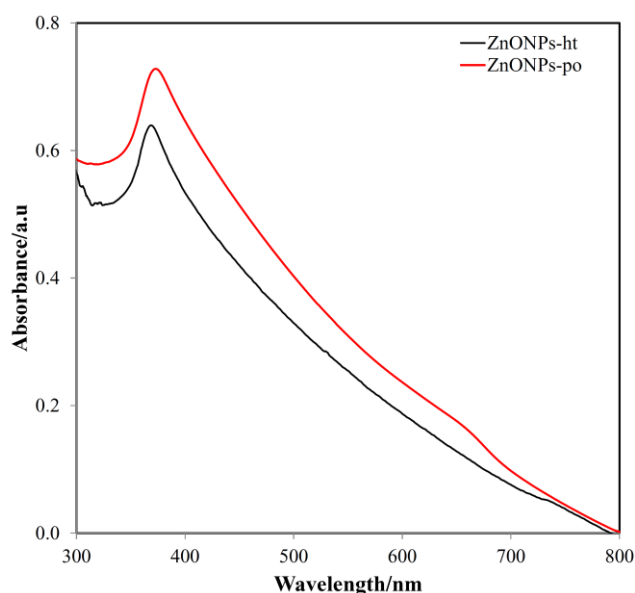


Figure 6 UV-Vis. absorption spectra of aqueous ZnONPs dispersions prepared by polyol and hydrothermal (150 °C) methods

#### 4. CONCLUSIONS

ZnONPs were successfully synthesized by using polyol and hydrothermal procedures. Hydrothermal synthesis was investigated for three different temperatures. SEM results revealed that polyol method presented formation of ball-shaped large particles including highly crystalline

hexagonal sub-units. Hydrothermal method produced small particles with aggregation at 100 and 120 °C but 150 °C exhibited screw-like large crystallites rather than small particles. The XRD analysis implied that polyol process yielded lower particle size than hydrothermal approach and particle size increased by rising the temperature of exposure for hydrothermal process. Band gap values of the ZnONPs products were calculated from UV-Vis. absorption data and found same as the bulk band gap value of 3.3 eV.

#### Funding

This study has been supported by Atatürk University Scientific Research Projects Coordination Unit. Project Number BAP FBA-2018/6920.

#### The Declaration of Conflict of Interest/ Common Interest

No conflict of interest or common interest has been declared by the authors.

#### Authors' Contribution

The authors contributed equally to the study

#### The Declaration of Ethics Committee Approval

The author declares that this document does not require an ethics committee approval or any special permission

#### The Declaration of Research and Publication Ethics

The authors of the paper declare that they comply with the scientific, ethical and quotation rules of SAUJS in all processes of the paper and that they do not make any falsification on the data collected. In addition, they declare that Sakarya University Journal of Science and its editorial board have no responsibility for any ethical violations that may be encountered, and that this study has not been evaluated in any academic

publication environment other than Sakarya University Journal of Science.

## REFERENCES

- [1] S. Kasap, İ. İ. Kaya, S. Repp, and E. Erdem, "Superbat: battery-like supercapacitor utilized by graphene foam and zinc oxide (ZnO) electrodes induced by structural defects," *Nanoscale Advances*, vol. 1, pp. 2586-2597, 2019.
- [2] M. M. Abutalib, and A. Rajeh, "Structural, thermal, optical and conductivity studies of Co/ZnO nanoparticles doped CMC polymer for solid state battery applications," *Polymer Testing*, vol. 91, pp. 106803, 2020.
- [3] B. Zhao, F. Mattelaer, J. Kint, A. Werbrouck, L. Henderick, M. Minjauw, J. Dendooven, and C. Detavernier, "Atomic layer deposition of ZnO-SnO<sub>2</sub> composite thin film: The influence of structure, composition and crystallinity on lithium-ion battery performance," *Electrochimica Acta*, vol. 320, pp. 134604, 2019.
- [4] A. Ali, M. Ammar, M. Ali, Z. Yahya, M. Y. Javaid, S. Hassan, and T. Ahmed, "Mo-doped ZnO nanoflakes on Ni-foam for asymmetric supercapacitor applications," *RSC Advances*, vol. 9, pp. 27432-27438, 2019.
- [5] S. Najib, F. Bakan, N. Abdullayeva, R. Bahariqushchi, S. Kasap, G. Franzò, M. Sankir, N. D. Sankir, S. Mirabella, and E. Erdem, "Tailoring morphology to control defect structures in ZnO electrodes for high-performance supercapacitor devices," *Nanoscale*, vol. 12, pp. 16162-16172, 2020.
- [6] N. P. Shetti, S. J. Malode, D. S. Nayak, G. B. Bagihalli, S. S. Kalanur, R. S. Malladi, C. V. Reddy, T. M. Aminabhavi, and K. R. Reddy, "Fabrication of ZnO nanoparticles modified sensor for electrochemical oxidation of methdilazine," *Applied Surface Science*, vol. 496, pp. 143656, 2019.
- [7] E. Erçarıkcı, and Murat Alanyalıoğlu, "Dual-functional Graphene-based flexible material for membrane filtration and electrochemical sensing of heavy metal ions", *IEEE Sensors Journal*, DOI 10.1109/JSEN.2020.3021988, 2020.
- [8] İ. Şişman, O. Tekir, and H. Karaca, "Role of ZnO photoanode nanostructures and sensitizer deposition approaches on the photovoltaic properties of CdS/CdSe and CdS<sub>1-x</sub>Se<sub>x</sub> quantum dot-sensitized solar cells," *Journal of Power Sources*, vol. 340, pp. 192-200, 2017.
- [9] İ. Şişman, M. Can, B. Ergezen, and M. Biçer, "One-step anion-assisted electrodeposition of ZnO nanofibrous networks as photoanodes for dye sensitized solar cells," *RSC Advances*, vol. 5, pp. 73692-73698, 2015.
- [10] X. Chen, G. Huang, C. An, R. Feng, Y. Wu, and C. Huang, "Plasma-induced PAA-ZnO coated PVDF membrane for oily wastewater treatment: preparation, optimization, and characterization through Taguchi OA design and synchrotron-based X-ray analysis," *Journal of Membrane Science*, vol. 582, pp. 70-82, 2019.
- [11] F. Naeem, S. Naeem, Z. Zhao, G. Shu, J. Zhang, Y. Mei, and G. Huang, "Atomic layer deposition synthesized ZnO nanomembranes: A facile route towards stable supercapacitor electrode for high capacitance," *Journal of Power Sources*, vol. 451, pp. 227740, 2020.
- [12] A. M. Qadir, I. Y. Erdogan, "Structural properties and enhanced photoelectrochemical performance of ZnO films decorated with Cu<sub>2</sub>O nanocubes," *International Journal of Hydrogen Energy*, vol. 44, pp. 18694-18702, 2019.
- [13] G. Utlu, "Structural investigation of ZnO thin films obtained by annealing after thermal evaporation," *Sakarya University Journal of Science*, vol. 23, pp. 650-656, 2019.

- [14] R. Mahdavi, and S. S. A. Talesh, "The effect of ultrasonic irradiation on the structure, morphology and photocatalytic performance of ZnO nanoparticles by sol-gel method," *Ultrasonics Sonochemistry*, vol. 39, pp. 504-510, 2017.
- [15] S. M. Li, L. X. Zhang, M. Y. Zhu, G. J. Ji, L. X. Zhao, J. Yin, and L. J. Bie, "Acetone sensing of ZnO nanosheets synthesized using room-temperature precipitation," *Sensors and Actuators B: Chemical*, vol. 249, pp. 611-623, 2017.
- [16] S. Lee, S. Jeong, D. Kim, S. Hwang, M. Jeon, and J. Moon, "ZnO nanoparticles with controlled shapes and sizes prepared using a simple polyol synthesis," *Superlattices and Microstructures*, vol. 43, pp. 330-339, 2008.
- [17] S. M. Saleh, A. M. Soliman, M. A. Sharaf, V. Kale, and B. Gadgil, "Influence of solvent in the synthesis of nano-structured ZnO by hydrothermal method and their application in solar-still," *Journal of Environmental Chemical Engineering*, vol. 5, pp. 1219-1226, 2017.
- [18] P. Kaur, S. Rani, and B. Lal, "Excitation dependent photoluminescence properties of ZnO nanophosphor," *Optik*, vol. 192, pp. 162929, 2019.
- [19] Ü. Ç. Üst, Ş. B. Demir, K. Dağcı, and M. Alanyalıoğlu, "Fabrication of free-standing graphene paper decorated with flower-like  $\text{PbSe}_{0.5}\text{S}_{0.5}$  structures," *RSC Advances*, vol. 6, pp. 9453-9460, 2016.
- [20] S. H. Largani, M. A. Pasha, "The effect of concentration ratio and type of functional group on synthesis of CNT-ZnO hybrid nanomaterial by an in situ sol-gel process," *International Nano Letters*, vol. 7, pp. 25-33, 2017.
- [21] T. Gutul, E. Rusu, N. Condur, V. Ursaki, E. Goncarenco, and P. Vlazan, "Preparation of poly(N-vinylpyrrolidone)-stabilized ZnO colloid nanoparticles," *Beilstein Journal of Nanotechnology*, vol. 5, pp. 402-406, 2014.
- [22] J. Singh, S. Kaur, G. Kaur, S. Basu, and M. Rawat, "Biogenic ZnO nanoparticles: a study of blueshift of optical band gap and photocatalytic degradation of reactive yellow 186 dye under direct sunlight," *Green Processing and Synthesis*, vol. 8, pp. 272-280, 2019.
- [23] T. Kasilingam, C. Thangavelu, and V. Palanivel, "Nano Analyses of Adsorbed Film onto Carbon Steel," *Portugaliae Electrochimica Acta*, vol. 32, pp. 259-270, 2014.
- [24] M. K. Debanath, S. Karmakar, "Study of blueshift of optical band gap in Zinc Oxide (ZnO) nanoparticles prepared by low temperature wet chemical method," *Materials Letters*, vol. 111, pp. 116-119, 2013.